

Electroless Deposition Metals on Poly(dimethylsiloxane) with Strong Adhesion As Flexible and Stretchable Conductive Materials

Fu-Tao Zhang,^{†,‡} Lu Xu,^{†,‡} Jia-Hui Chen,^{†,||} Bo Zhao,[†] Xian-Zhu Fu,^{*,†,§,¶} Rong Sun,^{*,†,¶} Qianwang Chen,[†] and Ching-Ping Wong^{#,□}

[†]Shenzhen Institutes of Advanced Technology, Chinese Academy of Sciences, Shenzhen, China

[‡]Institute of Nano Science and Technology, University of Science and Technology of China, Suzhou 215123, China

[§]College of Materials Science and Engineering, Shenzhen University, Shenzhen 518055, China

^{||}Shenzhen College of Advanced Technology, University of Chinese Academy of Sciences, Shenzhen 518055, P. R. China

[#]Hefei National Laboratory for Physical Sciences at Microscale and Department of Materials Science & Engineering, University of Science and Technology of China, Hefei 230026, China

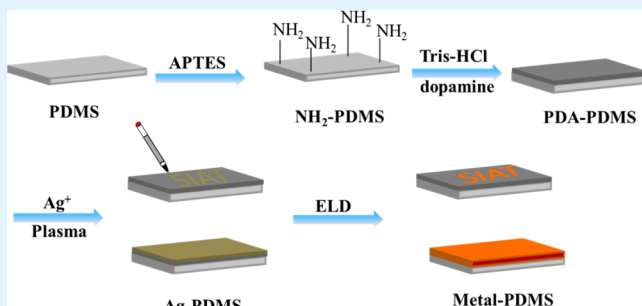
[¶]Department of Electronics Engineering, The Chinese University of Hong Kong, Hong Kong, China

[□]School of Materials Science and Engineering, Georgia Institute of Technology, Atlanta, Georgia 30332, United States

Supporting Information

ABSTRACT: A new surface modification method is developed for electroless deposition of robust metal (copper, nickel, silver) layers on poly(dimethylsiloxane) (PDMS) substrate with strong adhesion. Under the synergies of the polydopamine (PDA), the plasma process enhances Ag⁺ reduction, and a thin Ag film is capable of tightly attaching to the PDMS surface, which catalyzes electroless deposition (ELD) to form robust metal layers on the PDMS surface with strong adhesion. Subsequently, a flexible and stretchable Cu-PDMS conductor is obtained through this method, showing excellent metallic conductivity of $1.2 \times 10^7 \text{ S m}^{-1}$, even at the longest stretch strain (700%). This process provides a successful strategy for obtaining good robust metal layers on PDMS and other polymer substrate surfaces with strong adhesion and conductivity.

KEYWORDS: *poly(dimethylsiloxane), metal layers, polydopamine, plasma-treatment, flexible and stretchable conductor*



1. INTRODUCTION

Flexible and stretchable conductive materials play an important role in wearable devices.^{1–7} Metal material remains a primary choice because of its extremely high conductivity, appropriate price, and comparatively excellent stability. Crucially, metal is flexible when thin enough. What's more, metal is capable of folding or stretching when it is structured into proper shape.^{8,9}

Numerous methods of depositing metal films on flexible substrates have been reported, including physical vapor deposition (PVD),¹⁰ direct transfer metal precursors or metal nanoparticles onto polymer substrates,^{11,12} electroless deposition (ELD),^{13–15} electroplating,¹⁶ etc. PVD needs expensive equipment and complex operation steps. For direct transfer technology,¹⁷ relatively high annealing temperature has to be taken into account; in the meantime, high temperature may result in the damage of polymeric substrates and delamination of the metal. Electroplating is a commonly used technique in laboratory and industrial level. Nevertheless, the conductive substrate must be required, which is not suitable for most of the polymer substrate. In general, ELD is a good choice for the metallization of polymer surface with low cost and high conductivity. ELD is

an autocatalytic redox reaction to deposit thin layer metal film on a catalyst-preloaded substrate, which contains almost all of the flexible and rigid substrate. Besides, ELD can be carried out at room temperature without requirement of expensive equipment and with little, or even no damage to the substrate. Until now, ELD on a variety of flexible substrates, like cotton,¹⁸ paper,¹⁹ polyethylene terephthalate (PET), polyimide (PI),²⁰ and poly(vinylidene fluoride) (PVDF),²¹ etc., have been extensively studied. Pretreatment of substrates is very important for ELD. Polymer-assisted metal deposition (PAMD)²² is a strategy for fabricating flexible and stretchable metal conductors. A functional polymer layer has been innovatively introduced to promote the ELD on polymer substrates. Ligand-induced electroless plating (LIEP)²³ is primarily based on the “GraftFast” process to covalently graft a thin chelating polymer film, which can complex catalyst ion. Some other strategies, such as employing P4VP&SU-8 (the mixture of poly(4-vinylpyridine)

Received: October 16, 2017

Accepted: December 18, 2017

Published: December 18, 2017

and SU-8 in a certain proportion, SU-8 is a commercial photo-acid generator) as the strong bonding of polymer ligands to seize catalyst ion.²⁴ In essence, the purpose of these modifications is principally dependent on the formation of a thin film or functional group that easily adsorbs the catalyst ions on the surface of the flexible substrate.²⁵

Poly(dimethylsiloxane)(PDMS) belongs to a silicon-based organic elastomer, which has been the most widely used. Generally speaking, PDMS has many advantages, such as viscoelastic, chemically and mechanically robust, biocompatible, low cost and easily moldable. Benefiting from above characteristics, PDMS is satisfactory in actual application.²⁶ So far, it has been widely used in electronic, biomedical and chemical materials.^{9,27} Attributed to the superior performance of PDMS, tremendous research efforts have been paid to combine PDMS with conductive materials.^{28–33} For instance, conductive composites with elasticity have been formed by directly embedding conductive materials such as metal materials, carbon materials and conductive polymers into PDMS.^{34–36} Relative to the filled method, ELD of metal on the PDMS's surface^{37–39} has been widely used, owing to its many advantages. B. Carmichael et al. have combined microcontact printing with ELD to define a chemical pattern on the surface of PDMS.³⁸ Zheng et al. have reported that ELD on pre-strained PDMS surface for the fabrication of stretchable conductors by PAMD.²⁸ Görn et al. have reported site-selectivity ELD of silver on PDMS surface with the help of UV.³⁷ These method also have their shortcomings. For example, it is difficult to get a good combination for relying on APTES alone. And the polymer synthesis and relatively rigorous experimental environment are essential for PAMD. In addition, expensive equipment and costs are important factors that we must consider.

Herein, we propose a novel surface modification approach of PDMS for electroless deposition of metals (Cu, Ni, and Ag) with high adhesion as flexible and stretchable conductive conductors. The entire experimental procedure is facile, eliminating the need for expensive vacuum deposition and complex synthetic steps. Herein, polydopamine (PDA) as the bridge of PDMS and Ag^+ , can not only tightly absorb on the PDMS surface, but also promote the load and reduction of Ag^+ .⁴⁰ Plasma treatment enhances the Ag^+ reduction and a strong Ag catalyst film⁴⁰ can be formed on the surface of PDMS. Finally, ELD was performed on PDMS, leading to the formation of metal-coated PDMS. As proof-of-concept demonstration, we have successfully fabricated Cu-PDMS, Ni-PDMS and Ag-PDMS conductor. The as-made metal-PDMS showed high electrical conductivity, that is, 1.2×10^7 , 0.7×10^7 , and $1.8 \times 10^7 \text{ S m}^{-1}$, for Cu-PDMS, Ni-PDMS, and Ag-PDMS, respectively. Remarkably, we have designed a helical Cu-PDMS conductor for stretchable interconnect. The as-made Cu-PDMS (rectangular-shaped and helical-shaped) can remain stable metallic conductivity even under 5000 cycles at different deformation conditions. Besides, we further verify that the Cu-PDMS conductors are available for flexible and stretchable conductors to light up light-emitting diode (LED).

2. EXPERIMENTAL SECTION

2.1. Materials. PDMS prepolymer and curing agent (Sylgard 184) were purchased from Dow Corning. Dopamine hydrochloride ($\text{C}_8\text{H}_{11}\text{NO}_2\text{HCl}$), Tris (hydroxymethyl)-aminomethane, (3-aminopropyl)triethoxysilane (APTES, $\text{NH}_2(\text{CH}_2)_3\text{Si}(\text{OC}_2\text{H}_5)_3$), and all other chemicals were purchased from Aladdin.

2.2. Preparation of PDMS Film and Helical PDMS. PDMS films were prepared by curing a 10:1 mixture of PDMS prepolymer and curing agent on a precleaned glass ($10 \times 10 \text{ cm}^2$), and baking at 80°C for 2 h. Helical PDMS was made with the aid of a screw. As shown in Figure S8, the mixed PDMS without any bubbles was filled into the furrows of the screw. Then, the PDMS was cured at 80°C for 2 h. After that, the helical PDMS was gained by peeling it from the screw.

2.2.1. Preparation of the PDA Film on PDMS Substrate. The PDMS film was ultrasonically cleaned with acetone, ethanol and water for 15 min, respectively. Then, the PDMS film was put into 2% APTES solution with a mixture of ethanol and water ($m_{\text{ethanol}}:m_{\text{water}} = 95:5$) for 30 min. After that, the PDMS film was dried at 110°C for 20 min. Subsequently, the PDMS film was put into the Tris-HCl buffer, which contains 2 mg mL⁻¹ dopamine at pH = 8.5 for 24 h under stirring. Then, the substrate was ultrasonically cleaned with water and dried with N_2 flow.

2.2.2. Preparation of Silver Catalyst Ink. The silver catalyst ink was prepared by dissolving 5 mM silver nitrate (AgNO_3) in a 50 g mixture solution of ethanol and ethylene glycol in a ratio of 2:1 by weight.

2.2.3. Metallization by Electroless Deposition (ELD). The silver ion ink was spin-coated on the PDA-PDMS film. For the formation of "SIAT" logo pattern, the as-made Ag^+ ink was filled into the refill of a 0.7 mm ballpoint pen, and the Ag^+ ink traces were obtained by writing on PDA-PDMS surface. Subsequently, the Ag^+ -loaded PDMS substrate was exposed to atmosphere plasma for 30 min at 1000 mbar. Then, the PDMS substrate was immersed into the Cu plating bath which is composed of 1:1 mixture of freshly prepared solutions A and B. Solution A contains 15 g L^{-1} NaOH, 15 g L^{-1} $\text{K}_4[\text{Fe}(\text{CN})_6]$, 15 g L^{-1} $\text{CuSO}_4 \cdot 5\text{H}_2\text{O}$, 0.01 g L^{-1} $\text{K}_4\text{Fe}(\text{CN})_6 \cdot 3\text{H}_2\text{O}$. Solution B consists of 9.5 mL L^{-1} HCHO in water. The ELD of Ag was performed by first put Ag-PDMS substrate into the Cu ELD solution for several seconds, followed by immersing into the Ag plating bath ($1 \text{ g L}^{-1} [\text{Ag}(\text{H}_3\text{O})_2]\text{NO}_3$ and 5 g L^{-1} potassium sodium tartrate aqueous solution). ELD of Ni was conducted in the plating bath, which is composed of $\text{Ni}_2\text{SO}_4 \cdot 5\text{H}_2\text{O}$ (20 g L^{-1}), sodium citrate (33 g L^{-1}), sodium hypophosphite (14 g L^{-1}), and dimethylamine borane (DMAB) (3 g L^{-1}) in DI water, and the pH was adjusted to 10.0 with ammonia. After ELD, the substrate was dried under N_2 stream.

2.3. Characterization. The morphology and element analysis of PDMS with different modification were investigated by scanning electron microscopy (SEM, JSM-7800F and TEAM Octane Plus) coupled with EDS spectroscope. Atomic force microscopy (AFM, multimode-8, Bruker) was conducted in noncontact mode to characterize the surface morphology of different modification of PDMS. The resistances of metal coated-PDMS conductor was measured by Agilent 34401A. The conductivity of metal-PDMS was measured by using a 4-point probe method with a Keithley 2400 sourcemeter, where the measured distance was 1 cm. I-V characterization was measured by a Keithley 2400 Multimeter GPIB remote control.

3. RESULTS AND DISCUSSION

The fabrication of metal-PDMS conductors were schematically exhibited in Figure 1. In brief, precleaned elastomeric PDMS substrate was modified in 2% (3-aminopropyl)triethoxysilane (APTES, $\text{NH}_2(\text{CH}_2)_3\text{Si}(\text{OC}_2\text{H}_5)_3$) solution. APTES used here is a kind of NH₂-terminated trifunctional alkoxy silane ($\text{R}_0\text{Si}(\text{OR})_3$, where R and R₀ are methyl and aminopropyl groups, respectively), which acts as a molecular bridge between PDA and PDMS. After 30 min, the substrate was dried at 110°C for 20 min. In particular, this process has been repeated three times to improve modification effect of PDMS. Naturally, a thin film containing –NH₂ group was on the surface due to the hydrolysis of APTES. Fourier transform infrared Spectra was carried out to confirm the grafting result of APTES. As shown in Figure 2, –NH₂ vibration peaks at 3446 and 1635 cm⁻¹, respectively, indicated the successful grafting of APTES onto PDMS.

Polydopamine (PDA) is a polymer derived from dopamine,⁴¹ a bioglue that has been isolated from mussels. So far, PDA has

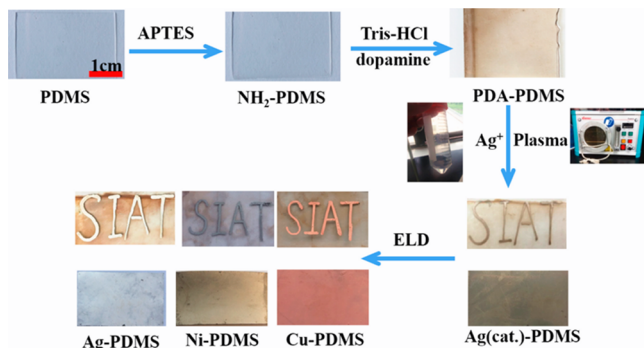


Figure 1. Scheme for the fabrication of metal–PDMS conductors.

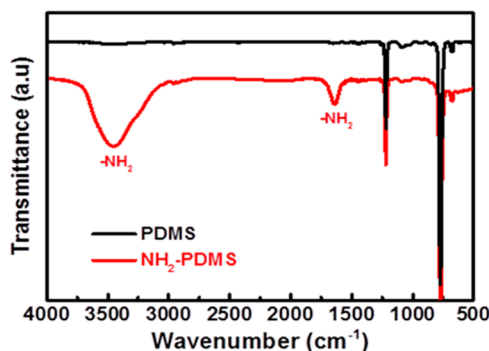


Figure 2. FT-IR spectra. Pristine PDMS (black line) and the same material after APTES grafting (red line).

been widely used as reductant, surface modification agent and binding agent, which attribute to its abundant active catechol, catechol, amine, and imine groups.^{42,43} Hence, it is responsible for their attachment to different surfaces in natural environment (e.g., rock).⁴⁴ Currently, the continuous PDA coatings can be synthesized on any object by including dopamine polymerization in a pure water phase or as suspended spherical nanoparticles in water–alcohol mixture at controlled pH. In the following step, the NH₂–PDMS film was transferred into the freshly prepared dopamine solution for 24 h under stirring. According to the previous researches about PDA,^{45,46} the ad-layer of –NH₂ can be formed on PDA surface by Schiff base or Michael addition reaction. Therefore, we can expect that PDA molecular could firmly attached to the NH₂–PDMS surface through chemical reaction. During the entire reaction process, the dopamine molecules were able to be chemically adsorbed onto the NH₂–PDMS surface and polymerized to form PDA. The detailed reaction mechanism is listed in the Figure S1. After the reaction, the PDA–PDMS was moved and dried in N₂ flow. At this moment, we observed that the PDMS surface was evenly darkened, suggesting the successful adsorption of PDA onto PDMS surface. Subsequently, the PDA–PDMS was immersed into the Ag⁺ ink for 10 min. Then the Ag–Ag⁺–PDMS substrate was placed into an atmosphere plasma machine for 30 min. Finally, the Ag–PDMS was immersed into Cu, Ni or Ag ELD solution, the Cu–PDMS, Ni–PDMS, Ag–PDMS and “SIAT” logo pattern (Figure 1) could be obtained. Table 1 has summarized the properties of the Cu, Ni and Ag on PDMS substrates. SEM images and Energy-dispersive X-ray spectroscopy (EDS) further confirmed the successful fabrication of Cu–PDMS, Ni–PDMS, and Ag–PDMS conductor. (Figure S3)

The SEM images in Figure 3 showed the evolution of surface topography of the PDMS film with different process.

Table 1. Summary of the Properties of Cu, Ni, and Ag on PDMS Substrates

metal-PDMS	thickness [μm]	resistance [mΩ]	conductivity [S m ⁻¹]
Cu	0.87 ± 0.09	203 ± 27	1.2 × 10 ⁷
Ni	1.16 ± 0.21	983 ± 125	0.7 × 10 ⁷
Ag	1.35 ± 0.19	115 ± 17	1.8 × 10 ⁷

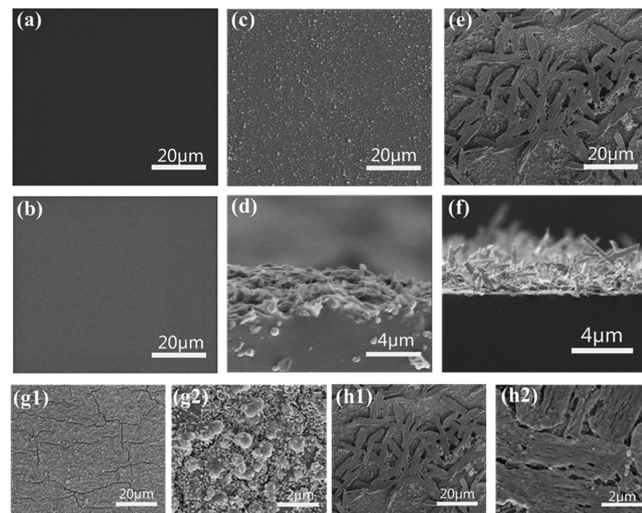


Figure 3. SEM images of different modification process: (a) Pristine PDMS, (b) NH₂–PDMS, surface (c) and cross-section (d) of PDA–PDMS, and surface (e) and cross-section (f) of Ag–PDMS, without (g1, g2) and with plasma treatment (h1, h2).

In contrast with the pristine PDMS surface (Figure 3a) and NH₂–PDMS (Figure 3b), the PDA–PDMS film was composed of small islets on the surface (Figure 3c). The uniform texture confirmed the conformal nature of PDA deposition. The cross-section SEM image (Figure 3d) also showed that some particles stacked on the surface of the PDMS substrate. As previously described, PDA was directly capable of reducing Ag⁺ into Ag⁰.⁴⁷ Hence, when the PDA–PDMS was immersed in Ag⁺ solution for 10 min, part of the silver ions could be reduced by the PDA. After that, more Ag⁺ ions were reduced into metal Ag particles with the aid of plasma. This inference was confirmed by comparing the morphology without and with plasma treatment (Figure 3g and 3h). As shown in Figure 3g1 and 3g2, the Ag particles from primary PDA reduction were granular-shaped. After plasma-treatment, the Ag layer was composed of granular-shaped and flake-shaped particles (Figure 3h1 and 3h2). Moreover, X-ray diffraction (XRD) was carried out to probe the surface of PDMS before and after plasma treatment. As shown in Figure S5, the XRD pattern was able to confirm the formation of Ag⁰ (JCPDS 04-0783). Therefore, we can be sure that Ag⁺ was reduced by plasma.

AFM was also used to analyze the topography of different processing steps. The pure PDMS surface exhibited flat surface with a few surface features and roughness of 2.67 nm (Figure 4a, e). Then, some of the protruding islands could be observed and the roughness reached 49.9 nm (Figure 4b, e), which indicated that APTES had successfully assembled on the PDMS surface to form a thin film. Many granular substances were appeared on the surface of PDMS after the adsorption of PDA particles (Figure 4c). Moreover, the AFM morphology of Ag–PDMS (Figure 4d) was accord with the SEM results in Figure 3e and 3f.

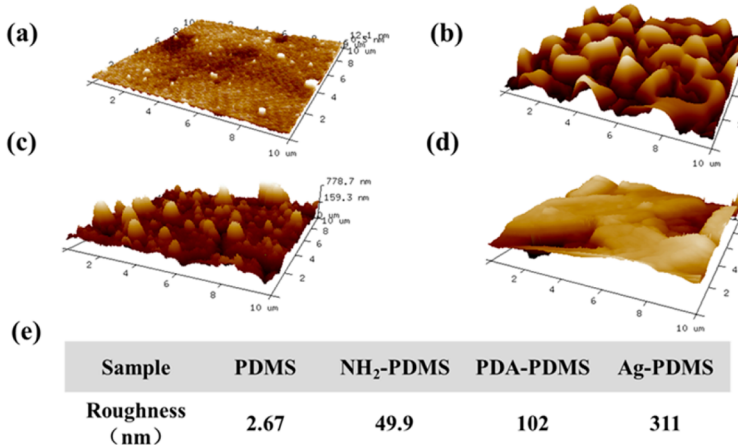


Figure 4. (a–d) AFM morphologies of different modification of PDMS (a) PDMS, (b) NH₂-PDMS, (c) PDA-PDMS, (d) Ag-PDMS, and (e) roughness of different modification of PDMS.

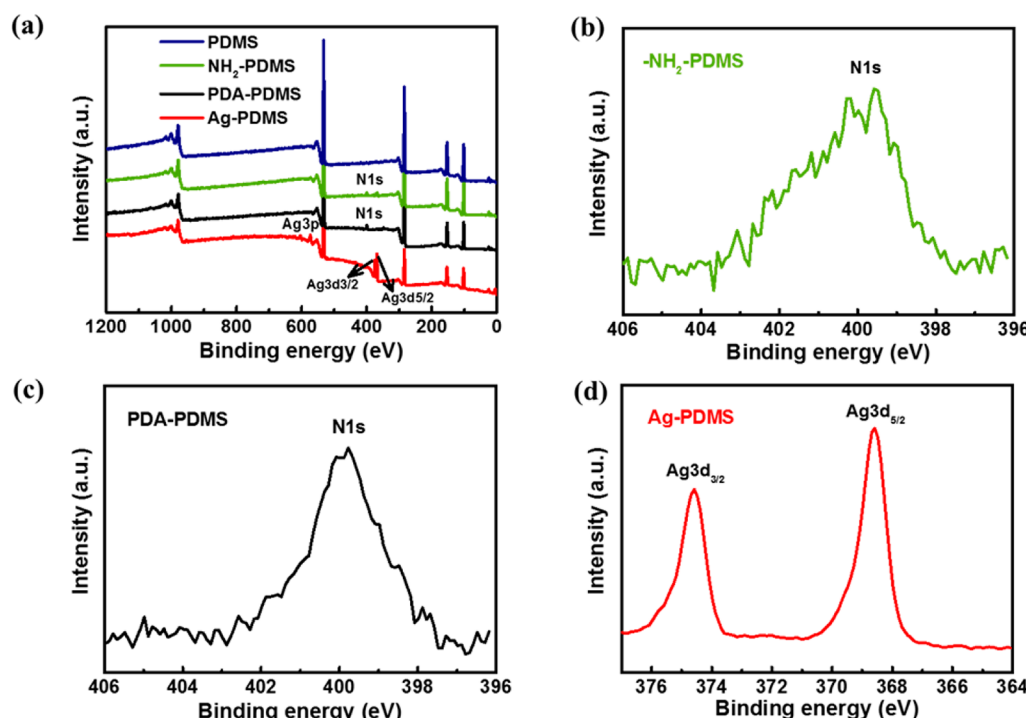


Figure 5. XPS (a) survey and high-resolution of (b) N 1s of NH₂-PDMS, (c) N 1s of PDA-PDMS, and (d) Ag 3d of Ag-PDMS.

X-ray photoelectron spectroscopy (XPS) was used for the surface characterization to precisely understand the surface components of PDMS film during the entire modification process. Figure 5a showed the survey spectra of PDMS in different modification steps. In comparison with pristine PDMS, additional N 1s peaks were found in NH₂-PDMS (Figure 5b) and PDA-PDMS (Figure 5c). In collaboration with the previous FT-IR result, we are confident in determining the successful adsorption of NH₂ on PDMS surface. Several characteristic Ag peaks (Figure 5a) were observed after the plasma treatment of Ag⁺-PDMS, and the two high resolution Ag 3d peaks were shown in Figure 5d.⁴⁸ It suggested the successful formation of Ag layer on the modified PDMS surface. Besides, from the EDS spectrum (Figure S2) of different modification process, we can also better understand the whole process through the changes in the types of elements. In addition, the comparisons between pristine PDMS and PDA-PDMS were

assessed by static water contact angle test (Figure S4). After modification, the water contact angle decreased from $50 \pm 10^\circ$ to $25 \pm 5^\circ$, which indicated that the hydrophilicity of the PDMS surface was improved by the PDA modification. This high hydrophilicity of PDA-PDMS was favorable for the adsorption of Ag⁺ and the subsequent reactions.

It should be noted that the PDA layer and plasma treatment play critical roles in the fabrication and final properties of the metal-PDMS conductors. Herein, PDA acted not only the reservoir of the Ag⁺ catalyst for facilitating the ELD process, but also the adhesion layer between the thin metal film and the substrate surface. We chose Cu as a model metal to study this issue. The previous literature^{46,47} reported that the PDA can behave as a reducing agent to reduce Ag⁺ to Ag⁰. Besides, the PDA can also act as a catalyst for ELD.⁴⁹ To more clearly understand the role of PDA and plasma treatment in the whole process. The without PDA, with PDA and Ag⁺ coated PDMS

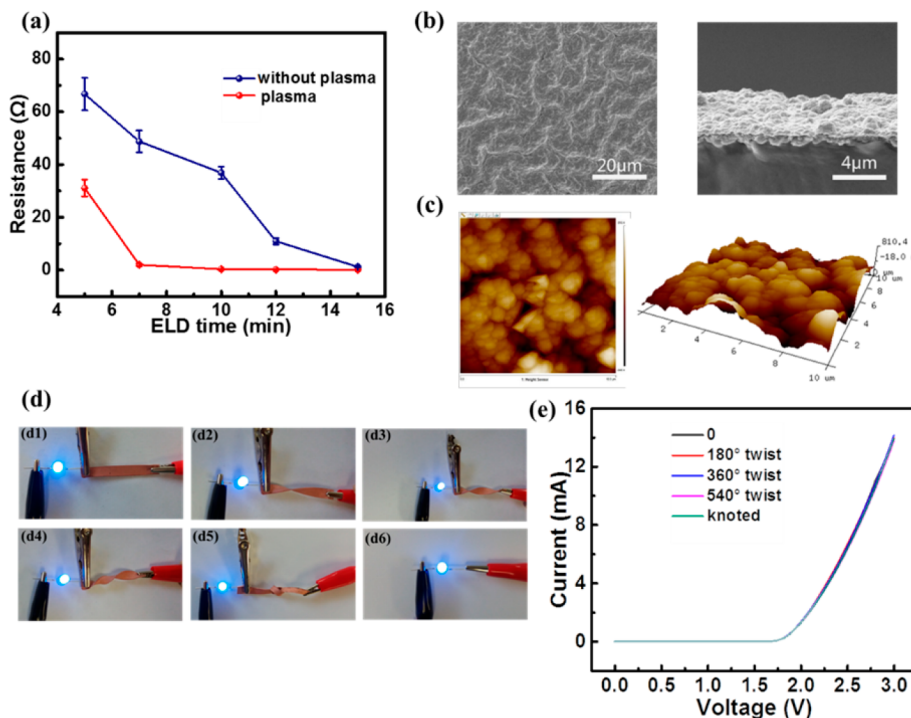


Figure 6. (a) The resistance variation of Cu layer obtained at various ELD time. (b) SEM images of surface morphologies of Cu layer and cross-section. (c) AFM image of Cu-PDMS. Digital images of LED-integrated circuit with the Cu-PDMS as interconnect. (d1–d6) is the original state, twisted 180°, 360°, 540°, knotted and without interconnect. (e) The I – V characteristics of the LED circuit (d) at different deformation condition.

(without plasma treatment) were subjected to ELD Cu process. A Cu layer can form on these three substrates, where the uses of PDA as a catalyst need longer time. As is well-known, the bonding force between metal layer and substrate was one of the core critical issues for ELD. Tape test^{23,50} was carried out to assess the adhesion between the deposited Cu layer and the PDMS substrate. As presented in Figure S6, a $1 \times 1 \text{ cm}^2$ area was divided into 100 square (10×10 ; $1 \times 1 \text{ mm}$ each). And a tape (Scotch600, 3M) was tightly adhered onto the surface of these lattices and then quickly peeled off vertically to the substrate. From Figure S6, the latticed Cu layer with plasma treatment (Figure S6d) got a score of 5B (the highest score according to ASTM D3359), which exhibited an excellent adhesion on the modified PDMS substrate. In addition, the effect of different plasma treatment times on Ag catalytic layer was investigated. Obviously, the amount of reduced Ag increased with increasing plasma processing time. At a short processing time shorter than 30 min, SEM images of Ag layer exhibited some cracks (Figure S7a–c) and could be easily wiped off, indicating the poor adhesion between the Ag layer and PDMS substrate. Whereas, when the time continues to increase, the effect Ag layer was not significantly improved. Thus, the plasma treatment time was optimized to 30 min.

During ELD, the resistance of the deposited Cu layer decreased with the increase of electroless deposition time (Figure 6a). In our experiments, we chose a $2 \times 1 \text{ cm}^2$ region of Cu-PDMS, and five different areas were selected to get average sheet resistances of Cu thin films. A conductive pattern with 2.013Ω could be gained after 7 min, and the resistance continue to decrease until the deposition time reached 15 min. In the meantime, by comparing the resistance-time variation curve, a smaller resistance value can be achieved in a shorter time by plasma-treatment (red line), which indicated that Ag^+ after plasma treatment have better catalytic efficiency. Attributed to

the PDA and plasma-treatment, from Figure 6b and 6c, the obtained Cu layer was densely arranged without gaps. As proof-of-concept for the application of the as-made Cu-PDMS conductor, we lighted a commercially available light-emitting diode (LED) with the as-made Cu-PDMS conductor. In the meanwhile, the current–voltage (I – V) characteristics were measured when the circuit was 0, 180°, 360°, 540° twist and knotted. Significantly, the I – V characteristics curves also overlap for different twists of the substrate, indicating the resistances of the Cu-PDMS conductor almost did not change. On the basis of this unique feature of Cu-PDMS, we continued to carry out other studies to verify its high conductivity. As depicted in Figure 7a, the Cu-PDMS conductor was bent to different radius of curvatures (r , mm) until the Cu-PDMS was folded. The normalized resistance (R/R_0), maintained stable at 1.0 until r reached 8.0 mm, afterward gradually increase to 1.50 until 2.2 mm, in which R_0 is the resistance of the conductor before testing. Simultaneously, the normalized resistance (R/R_0) test was also carried out at different bending angles. The Figure 7b showed the Cu-PDMS were folded to -180° , -135° , -90° , -45° (negative angles indicate folding of the Cu-PDMS out-plane) and 45° , 90° , 135° , 180° (positive angles indicate folding of the Cu-PDMS in-plane). It can be seen that when the substrate was folded -180° or 180° , the normalized resistance reached the maximum. Moreover, fatigue tests were conducted at different bending radius (1, 5 mm) and angles (45° , 90° , 135°) for 5000 cycles. The results demonstrate that the resistance at each step of deformation does not show obvious changes (Figure 7a–c). Therefore, the Cu-PDMS was capable of a desired interconnect for flexible electronic applications.

PDMS precursor has a strong plasticity, it can be easily processed into a variety of shapes after curing. PDMS is a good choice for stretchable conductor. For stretchable conductors, it has been achieved by developing “materials that stretch” or

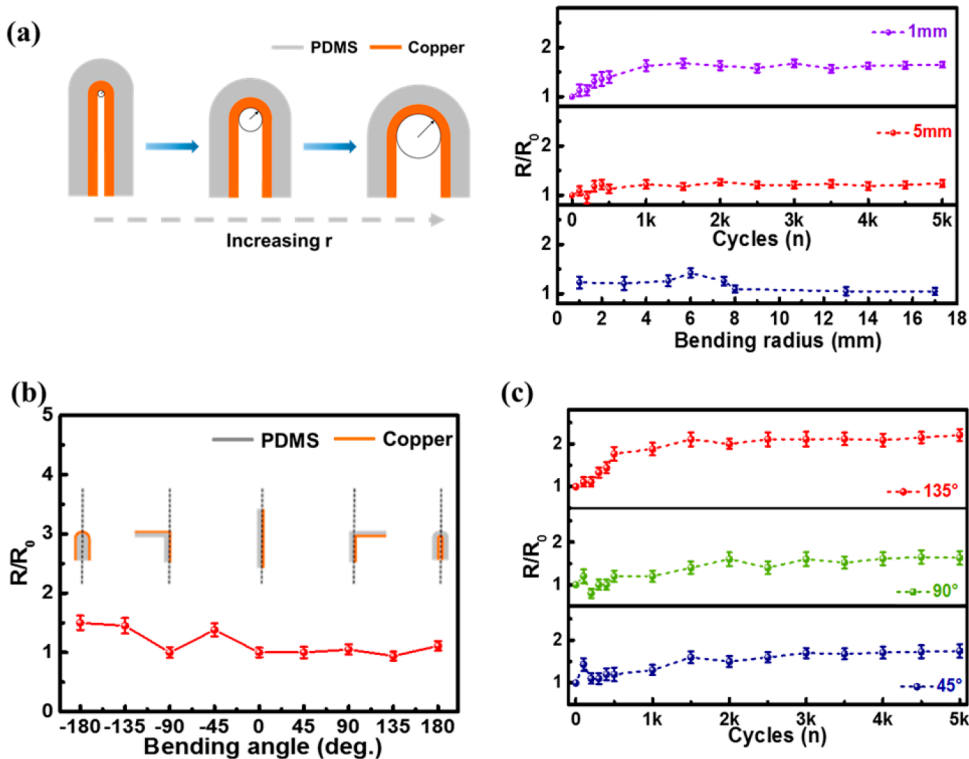


Figure 7. (a) Normalized resistance of Cu-PDMS at different bending radii and fatigue tests of bendability. (b) Normalized resistances of Cu-PDMS at different bending angle. (c) Fatigue test of bending angles at 45°, 90°, and 135°.

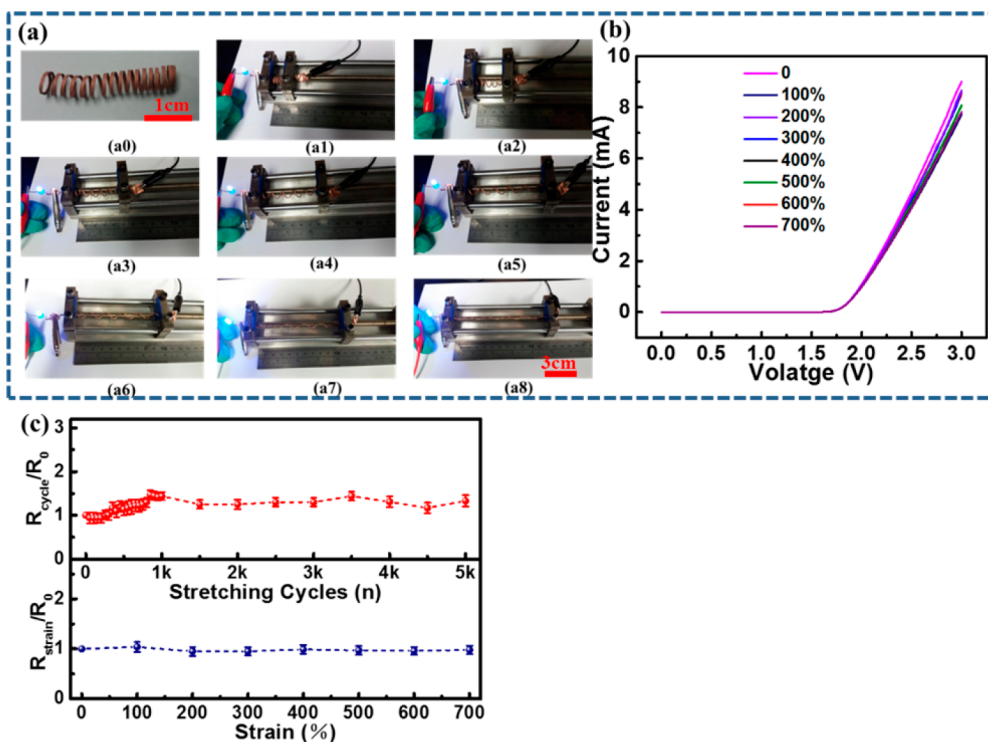


Figure 8. (a) Helical-shape Cu-PDMS stretchable conductor (a_0), the LED-integrated circuit with Cu-PDMS conductor at 1.5 (origin), 3 (100%), 4.5 (200%), 6 (300%), 7.5 (400%), 9 (500%), 10.5 (600%), 12 cm (700%), respectively (a_1-a_8) (see Supporting Movie S1 for the operation of this helical conductor). (b) The $I-V$ characteristics of the LED circuit (d) at different deformation condition. (c) Fatigue test at 700% stretch (red line) and normalized resistance of Cu-PDMS stretchable conductor different tensile strains.

"structures that stretch" strategies.^{9,28,51} When the PDMS is designed to certain structures, it will possess better stretchability (the electrical and mechanical performance of PDMS

and Cu-PDMS are shown in Figure S9). Helical structure is a common structure in our daily life, which spans from telephone cords and springs to DNA and climbing plants.⁵² Herein, a

spring-like elastic conductor was made by PDMS and ELD Cu coating. The specific fabrication process was shown in Figure S8. To figure out the stretchability of this helical-shaped Cu-PDMS, we fixed it on self-designed mold integrated with an external circuit. As shown in Figure 8a1–a8, when the helical Cu-PDMS at initial state, the initial length of the conductor (1.5 cm) was defined as 0%. Moreover, when it was stretched to 3 (100%), 4.5 (200%), 6 (300%), 7.5 (400%), 9 (500%), 10.5 (600%), and 12 cm (700%), respectively, the LED light could work properly. The *I*-*V* characteristics of the circuits showed some variation upon stretching of the Cu-PDMS interconnects, which agreed well with the stretching tests (Figure 8b and 8c). More importantly, the R/R_0 roughly maintained at 1.0 while the spring-like conductor was stretched to the longest statue in the fatigue tests (Figure 8c).

4. CONCLUSIONS

A novel and facile surface modification method of PDMS has been introduced for electroless deposition of metal with strong adhesion. The PDA modified layer and plasma enhanced Ag⁺ reduction is responsible for the successful assembly of a flexible and stretchable conductor. The PDA layer serve as a solid bridge between PDMS substrate and Ag⁺ catalyst ink, absorbing Ag⁺ and partially reducing Ag⁺ into Ag nanoparticles. Consequently, plasma treatment further enhanced the reduction and adsorption of the Ag⁺ catalyst. A flexible and stretchable Cu-PDMS conductor is obtained by using this method, showing excellent metallic conductivity of $1.2 \times 10^7 \text{ S m}^{-1}$, even at longest stretch strain (700%).

■ ASSOCIATED CONTENT

Supporting Information

The Supporting Information is available free of charge on the ACS Publications website at DOI: [10.1021/acsami.7b15726](https://doi.org/10.1021/acsami.7b15726).

Formation process of PDA–PDMS, EDS of different modification, SEM and EDS of metal–PDMS, contact angle of water on the surface of PDMS and PDA–PDMS, XRD of Ag-PDMS, 3 M tape test, SEM of Ag-PDMS at different plasma-treatment times, fabrication process for the helical-structured Cu conductor, and electrical and mechanical performance of PDMS and Cu-PDMS ([PDF](#))
Operation of this helical conductor ([AVI](#))

■ AUTHOR INFORMATION

Corresponding Authors

*E-mail: xz.fu@szu.edu.cn. Tel: +86-755-86392151. Fax: +86-755-86392299.

*E-mail: rong.sun@siat.ac.cn.

ORCID

Xian-Zhu Fu: [0000-0003-1843-8927](https://orcid.org/0000-0003-1843-8927)

Rong Sun: [0000-0001-9719-3563](https://orcid.org/0000-0001-9719-3563)

Notes

The authors declare no competing financial interest.

■ ACKNOWLEDGMENTS

This work was financially supported by the National Natural Science Foundation of China (No. 21203236), Guangdong Department of Science and Technology (2017A050501052), Guangdong Provincial Laboratory of Key Materials for High Density Electronic Packaging (2014B030301014), and Shenzhen basic research plan (JCYJ20160229195455154).

■ REFERENCES

- (1) Yan, Y.; Warren, S. C.; Fuller, P.; Grzybowski, B. A. Chemoelectronic circuits based on metal nanoparticles. *Nat. Nanotechnol.* **2016**, *11*, 603–608.
- (2) Tee, B. C.; Wang, C.; Allen, R.; Bao, Z. An electrically and mechanically self-healing composite with pressure- and flexion-sensitive properties for electronic skin applications. *Nat. Nanotechnol.* **2012**, *7*, 825–832.
- (3) Yang, Y.; Huang, Q.; Niu, L.; Wang, D.; Yan, C.; She, Y.; Zheng, Z. Waterproof, Ultrahigh Areal-Capacitance, Wearable Supercapacitor Fabrics. *Adv. Mater.* **2017**, *29*, 1606679.
- (4) Gao, W.; Emaminejad, S.; Nyein, H. Y. Y.; Challa, S.; Chen, K.; Peck, A.; Fahad, H. M.; Ota, H.; Shiraki, H.; Kiriya, D.; Lien, D. H.; Brooks, G. A.; Davis, R. W.; Javey, A. Fully integrated wearable sensor arrays for multiplexed in situ perspiration analysis. *Nature* **2016**, *529*, 509–514.
- (5) Oh, J. Y.; Rondeau-Gagne, S.; Chiu, Y. C.; Chortos, A.; Lissel, F.; Wang, G. N.; Schroeder, B. C.; Kurosawa, T.; Lopez, J.; Katsumata, T.; Xu, J.; Zhu, C.; Gu, X.; Bae, W. G.; Kim, Y.; Jin, L.; Chung, J. W.; Tok, J. B.; Bao, Z. Intrinsically stretchable and healable semiconducting polymer for organic transistors. *Nature* **2016**, *539*, 411–415.
- (6) Qi, D.; Liu, Z.; Liu, Y.; Jiang, Y.; Leow, W. R.; Pal, M.; Pan, S.; Yang, H.; Wang, Y.; Zhang, X.; Yu, J.; Li, B.; Yu, Z.; Wang, W.; Chen, X. Highly Stretchable, Compliant, Polymeric Microelectrode Arrays for In Vivo Electrophysiological Interfacing. *Adv. Mater.* **2017**, *29*, 1702800.
- (7) Liu, Z. F.; Fang, S.; Moura, F. A.; Ding, J. N.; Jiang, N.; Di, J.; Zhang, M.; Lepro, X.; Galvao, D. S.; Haines, C. S.; Yuan, N. Y.; Yin, S. G.; Lee, D. W.; Wang, R.; Wang, H. Y.; Lv, W.; Dong, C.; Zhang, R. C.; Chen, M. J.; Yin, Q.; Chong, Y. T.; Zhang, R.; Wang, X.; Lima, M. D.; Ovalle-Robles, R.; Qian, D.; Lu, H.; Baughman, R. H. Hierarchically buckled sheath-corefibers for superelastic electronics, sensors, and muscles. *Science* **2015**, *349*, 400–404.
- (8) Kim, D. H.; Xiao, J.; Song, J.; Huang, Y.; Rogers, J. A. Stretchable, curvilinear electronics based on inorganic materials. *Adv. Mater.* **2010**, *22*, 2108–2124.
- (9) Rogers, J. A.; Someya, T.; Huang, Y. Materials and Mechanics for Stretchable Electronics. *Science* **2010**, *327*, 1603.
- (10) Selvakumar, N.; Barshilia, H. C. Review of physical vapor deposited (PVD) spectrally selective coatings for mid- and high-temperature solar thermal applications. *Sol. Energy Mater. Sol. Cells* **2012**, *98*, 1–23.
- (11) Park, M.; Im, J.; Shin, M.; Min, Y.; Park, J.; Cho, H.; Park, S.; Shim, M. B.; Jeon, S.; Chung, D. Y.; Bae, J.; Park, J.; Jeong, U.; Kim, K. Highly stretchable electric circuits from a composite material of silver nanoparticles and elastomeric fibres. *Nat. Nanotechnol.* **2012**, *7*, 803–809.
- (12) Jeon, J.; Lee, H. B.; Bao, Z. Flexible wireless temperature sensors based on Ni microparticle-filled binary polymer composites. *Adv. Mater.* **2013**, *25*, 850–855.
- (13) Yu, Y.; Zeng, J.; Chen, C.; Xie, Z.; Guo, R.; Liu, Z.; Zhou, X.; Yang, Y.; Zheng, Z. Three-dimensional compressible and stretchable conductive composites. *Adv. Mater.* **2014**, *26*, 810–815.
- (14) Azzaroni, O.; Zheng, Z.; Yang, Z.; Huck, W. T. Polyelectrolyte brushes as efficient ultrathin platforms for site-selective copper electroless deposition. *Langmuir* **2006**, *22*, 6730–6733.
- (15) Guo, R.; Yu, Y.; Xie, Z.; Liu, X.; Zhou, X.; Gao, Y.; Liu, Z.; Zhou, F.; Yang, Y.; Zheng, Z. Matrix-assisted catalytic printing for the fabrication of multiscale, flexible, foldable, and stretchable metal conductors. *Adv. Mater.* **2013**, *25*, 3343–3350.
- (16) Abbott, A. P.; McKenzie, K. J. Application of ionic liquids to the electrodeposition of metals. *Phys. Chem. Chem. Phys.* **2006**, *8*, 4265–4279.
- (17) Kanzaki, M.; Kawaguchi, Y.; Kawasaki, H. Fabrication of Conductive Copper Films on Flexible Polymer Substrates by Low-Temperature Sintering of Composite Cu Ink in Air. *ACS Appl. Mater. Interfaces* **2017**, *9*, 20852–20858.
- (18) Liu, X.; Chang, H.; Li, Y.; Huck, W. T.; Zheng, Z. Polyelectrolyte-bridged metal/cotton hierarchical structures for highly

- durable conductive yarns. *ACS Appl. Mater. Interfaces* **2010**, *2*, 529–535.
- (19) Wang, Y.; Guo, H.; Chen, J. J.; Sowade, E.; Wang, Y.; Liang, K.; Marcus, K.; Baumann, R. R.; Feng, Z. S. Paper-Based Inkjet-Printed Flexible Electronic Circuits. *ACS Appl. Mater. Interfaces* **2016**, *8*, 26112–26118.
- (20) Liao, Y. C.; Kao, Z. K. Direct writing patterns for electroless plated copper thin film on plastic substrates. *ACS Appl. Mater. Interfaces* **2012**, *4*, 5109–5113.
- (21) Voet, V. S.; Tichelaar, M.; Tanase, S.; Mittelmeijer-Hazeleger, M. C.; ten Brinke, G.; Loos, K. Poly(vinylidene fluoride)/nickel nanocomposites from semicrystalline block copolymer precursors. *Nanoscale* **2013**, *5*, 184–192.
- (22) Yu, Y.; Yan, C.; Zheng, Z. Polymer-assisted metal deposition (PAMD): a full-solution strategy for flexible, stretchable, compressible, and wearable metal conductors. *Adv. Mater.* **2014**, *26*, 5508–5516.
- (23) Garcia, A.; Polesel-Maris, J.; Viel, P.; Palacin, S.; Berthelot, T. Localized Ligand Induced Electroless Plating (LIEP) Process for the Fabrication of Copper Patterns Onto Flexible Polymer Substrates. *Adv. Funct. Mater.* **2011**, *21*, 2096–2102.
- (24) Hu, M.; Guo, Q.; Zhang, T.; Zhou, S.; Yang, J. SU-8-Induced Strong Bonding of Polymer Ligands to Flexible Substrates via in Situ Cross-Linked Reaction for Improved Surface Metallization and Fast Fabrication of High-Quality Flexible Circuits. *ACS Appl. Mater. Interfaces* **2016**, *8*, 4280–4286.
- (25) Li, B.; Yu, B.; Ye, Q.; Zhou, F. Tapping the potential of polymer brushes through synthesis. *Acc. Chem. Res.* **2015**, *48*, 229–237.
- (26) Mata, A.; Fleischman, A. J.; Roy, a. S. Characterization of Polydimethylsiloxane (PDMS) Properties for Biomedical Micro/Nanosystems. *Biomed. Biomed. Microdevices* **2005**, *7*, 281–293.
- (27) Magennis, E. P.; Hook, A. L.; Williams, P.; Alexander, M. R. Making Silicone Rubber Highly Resistant to Bacterial Attachment Using Thiol-ene Grafting. *ACS Appl. Mater. Interfaces* **2016**, *8*, 30780–30787.
- (28) Wang, X.; Hu, H.; Shen, Y.; Zhou, X.; Zheng, Z. Stretchable conductors with ultrahigh tensile strain and stable metallic conductance enabled by prestrained polyelectrolyte nanoplates. *Adv. Mater.* **2011**, *23*, 3090–3094.
- (29) Wang, M.; Zhang, K.; Dai, X. X.; Li, Y.; Guo, J.; Liu, H.; Li, G. H.; Tan, Y. J.; Zeng, J. B.; Guo, Z. Enhanced electrical conductivity and piezoresistive sensing in multi-wall carbon nanotubes/polydimethylsiloxane nanocomposites via the construction of a self-segregated structure. *Nanoscale* **2017**, *9*, 11017–11026.
- (30) Bae, G. Y.; Pak, S. W.; Kim, D.; Lee, G.; Kim, D. H.; Chung, Y.; Cho, K. Linearly and Highly Pressure-Sensitive Electronic Skin Based on a Bioinspired Hierarchical Structural Array. *Adv. Mater.* **2016**, *28*, 5300–5306.
- (31) Lipomi, D. J.; Lee, J. A.; Vosgueritchian, M.; Tee, B. C. K.; Bolander, J. A.; Bao, Z. Electronic Properties of Transparent Conductive Films of PEDOT: PSS on Stretchable Substrates. *Chem. Mater.* **2012**, *24*, 373–382.
- (32) Li, X.; Cai, J.; Shi, Y.; Yue, Y.; Zhang, D. Remarkable Conductive Anisotropy of Metallic Microcoil/PDMS Composites Made by Electric Field Induced Alignment. *ACS Appl. Mater. Interfaces* **2017**, *9*, 1593–1601.
- (33) Duan, S.; Wang, Z.; Zhang, L.; Liu, J.; Li, C. Three-Dimensional Highly Stretchable Conductors from Elastic Fiber Mat with Conductive Polymer Coating. *ACS Appl. Mater. Interfaces* **2017**, *9*, 30772–30778.
- (34) Jiang, J.; Bao, B.; Li, M.; Sun, J.; Zhang, C.; Li, Y.; Li, F.; Yao, X.; Song, Y. Fabrication of Transparent Multilayer Circuits by Inkjet Printing. *Adv. Mater.* **2016**, *28*, 1420–1426.
- (35) Chen, M.; Zhang, L.; Duan, S.; Jing, S.; Jiang, H.; Li, C. Highly Stretchable Conductors Integrated with a Conductive Carbon Nanotube/Graphene Network and 3D Porous Poly(dimethylsiloxane). *Adv. Funct. Mater.* **2014**, *24*, 7548–7556.
- (36) Wu, S.; Zhang, J.; Ladani, R. B.; Ravindran, A. R.; Mouritz, A. P.; Kinloch, A. J.; Wang, C. H. Novel Electrically Conductive Porous PDMS/Carbon Nanofiber Composites for Deformable Strain Sensors and Conductors. *ACS Appl. Mater. Interfaces* **2017**, *9*, 14207–14215.
- (37) Polywka, A.; Jakob, T.; Stegers, L.; Riedl, T.; Gorrn, P. Facile preparation of high-performance elastically stretchable interconnects. *Adv. Mater.* **2015**, *27*, 3755–3759.
- (38) Miller, M. S.; Davidson, G. J. E.; Sahli, B. J.; Mailloux, C. M.; Carmichael, T. B. Fabrication of Elastomeric Wires by Selective Electroless Metallization of Poly(dimethylsiloxane). *Adv. Mater.* **2008**, *20*, 59–64.
- (39) Molazemhosseini, A.; Ieffa, S.; Vena, P.; Magagnin, L. SAM Assisted Nickel-Boron Electroless Metallization of PDMS. *ECS Trans.* **2015**, *66*, 13–22.
- (40) Liu, S.; Tao, H.; Zeng, L.; Liu, Q.; Xu, Z.; Liu, Q.; Luo, J. L. Shape-Dependent Electrocatalytic Reduction of CO₂ to CO on Triangular Silver Nanoplates. *J. Am. Chem. Soc.* **2017**, *139*, 2160–2163.
- (41) Lee, H.; Dellatore, S. M.; Miller, W. M.; Messersmith, P. B. Mussel-inspired surface chemistry for multifunctional coatings. *Science* **2007**, *318*, 426–430.
- (42) Cong, Y.; Xia, T.; Zou, M.; Li, Z.; Peng, B.; Guo, D.; Deng, Z. Mussel-inspired polydopamine coating as a versatile platform for synthesizing polystyrene/Ag nanocomposite particles with enhanced antibacterial activities. *J. Mater. Chem. B* **2014**, *2*, 3450–3461.
- (43) Liu, Y.; Ai, K.; Liu, J.; Deng, M.; He, Y.; Lu, L. Dopamine-melanin colloidal nanospheres: an efficient near-infrared photothermal therapeutic agent for in vivo cancer therapy. *Adv. Mater.* **2013**, *25*, 1353–1359.
- (44) Akter, T.; Kim, W. S. Reversibly stretchable transparent conductive coatings of spray-deposited silver nanowires. *ACS Appl. Mater. Interfaces* **2012**, *4*, 1855–1859.
- (45) Sileika, T. S.; Kim, H. D.; Maniak, P.; Messersmith, P. B. Antibacterial performance of polydopamine-modified polymer surfaces containing passive and active components. *ACS Appl. Mater. Interfaces* **2011**, *3*, 4602–4610.
- (46) Liu, Y.; Ai, K.; Lu, L. Polydopamine and Its Derivative Materials: Synthesis and Promising Applications in Energy, Environmental, and Biomedical Fields. *Chem. Rev.* **2014**, *114*, 5057–5115.
- (47) Niu, H.; Wang, S.; Zeng, T.; Wang, Y.; Zhang, X.; Meng, Z.; Cai, Y. Preparation and characterization of layer-by-layer assembly of thiols/Ag nanoparticles/polydopamine on PET bottles for the enrichment of organic pollutants from water samples. *J. Mater. Chem.* **2012**, *22*, 15644–15653.
- (48) Jin, Y.; Cheng, Y.; Deng, D.; Jiang, C.; Qi, T.; Yang, D.; Xiao, F. Site-selective growth of patterned silver grid networks as flexible transparent conductive film by using poly(dopamine) at room temperature. *ACS Appl. Mater. Interfaces* **2014**, *6*, 1447–1453.
- (49) Ma, S.; Liu, L.; Bromberg, V.; Singler, T. J. Electroless copper plating of inkjet-printed polydopamine nanoparticles: a facile method to fabricate highly conductive patterns at near room temperature. *ACS Appl. Mater. Interfaces* **2014**, *6*, 19494–19498.
- (50) Wang, Y.; Wang, Y.; Chen, J.-j.; Guo, H.; Liang, K.; Marcus, K.; Peng, Q.-l.; Zhang, J.; Feng, Z.-s. A facile process combined with inkjet printing, surface modification and electroless deposition to fabricate adhesion-enhanced copper patterns on flexible polymer substrates for functional flexible electronics. *Electrochim. Acta* **2016**, *218*, 24–31.
- (51) Sun, Y.; Rogers, J. A. Structural forms of single crystal semiconductor nanoribbons for high-performance stretchable electronics. *J. Mater. Chem.* **2007**, *17*, 832.
- (52) Won, Y.; Kim, A.; Yang, W.; Jeong, S.; Moon, J. A highly stretchable, helical copper nanowire conductor exhibiting a stretchability of 700%. *NPG Asia Mater.* **2014**, *6*, e132.

Electroless Deposition Metals on Poly(dimethylsiloxane) with Strong Adhesion As Flexible and Stretchable Conductive Materials

Zhang, Fu Tao; Xu, Lu; Chen, Jia Hui; Zhao, Bo; Fu, Xian Zhu; Sun, Rong; Chen, Qianwang; Wong, Ching Ping

- 01 shuo zhang Page 1
22/4/2022 2:42
- 02 shuo zhang Page 1
22/4/2022 2:26
- 03 shuo zhang Page 2
11/5/2022 13:57
- 04 shuo zhang Page 2
11/5/2022 13:57
- 05 shuo zhang Page 2
1/5/2022 23:09
- 06 shuo zhang Page 2
13/6/2022 14:23
- 07 shuo zhang Page 3
22/4/2022 2:28